Breast Cancer: Targets and Therapy

Dovepress
Taylor & Francis Group

Open Access Full Text Article

ORIGINAL RESEARCH

Development and Validation of a Radiomics-Based Nomogram for Predicting HER-2 Status in Breast Cancer: A Retrospective Study with Small Validation Cohort

Qingxiang Qiu[1,*], Chajin Chen[1,*], Jinyin Chen[1], Chuntao Liao[2], Langlang Tang[1]

[1]Department of Radiology, Longyan First Affiliated Hospital of Fujian Medical University, Longyan, Fujian, 364000, People's Republic of China; [2]Department of Thyroid and Breast Surgery, Longyan First Affiliated Hospital of Fujian Medical University, Longyan, Fujian, 364000, People's Republic of China

*These authors contributed equally to this work

Correspondence: Langlang Tang, Department of Radiology, Longyan First Affiliated Hospital of Fujian Medical University, No. 105 Jiuyi North Load, Xinluo District, Longyan, Fujian, 364000, People's Republic of China, Tel +86 0597 2205060, Email tanglanglangdr@126.com

Aim: To develop and validate a radiomics-based nomogram using multimodal magnetic resonance imaging (MRI) features to predict HER-2 expression status in breast cancer.

Methods: A total of 320 breast cancer patients were retrospectively selected for this study, with 80 in the HER-2 positive group and 240 in the HER-2 negative group. Pre-treatment multimodal MRI scans, including dynamic contrast-enhanced MRI (DCE-MRI), diffusion-weighted imaging (DWI), and T2-weighted imaging, were used to extract radiomic features. Multivariate logistic regression was performed to identify independent predictors for HER-2 positivity. A radiomics-based nomogram was constructed and validated using both training and validation sets. The nomogram's performance was assessed using receiver operating characteristic (ROC) curve analysis and decision curve analysis (DCA).

Results: Multivariate analysis identified several independent predictors of HER-2 positivity, including type, edge, local skin thickening or depression, and axillary lymph node enlargement. The radiomics-based nomogram demonstrated excellent predictive accuracy with an area under the ROC curve (AUC) of 0.866 in the training set and 0.876 in the validation set. Calibration plots confirmed the model's good consistency, and DCA indicated that the nomogram provides significant clinical benefit across a range of threshold probabilities. In addition, the HER-2 positive group showed significantly higher tumor marker expression and immune cell infiltration, including elevated CD8+ T-cells, M1 macrophages, Tregs, and TAM ($p<0.001$).

Conclusion: The radiomics-based nomogram developed in this study offers a promising non-invasive tool for predicting HER-2 expression status in breast cancer. By integrating clinical data and advanced MRI features, this model provides accurate predictions, improving personalized treatment strategies. Further validation in larger, multicenter studies is necessary to confirm its generalizability and clinical applicability.

Keywords: radiomics, HER-2, breast cancer, MRI, nomogram

Introduction

Breast cancer remains one of the most prevalent and challenging malignancies globally, with significant public health implications.[1] The human epidermal growth factor receptor 2 (HER-2) status plays a crucial role in determining the aggressiveness of the tumor and guiding treatment decisions.[2] HER-2 overexpression, observed in 15–20% of breast cancer cases,[3] is linked to a poorer prognosis and higher likelihood of recurrence,[4] making accurate HER-2 assessment essential for personalized therapy, especially when selecting HER-2-targeted treatments such as trastuzumab. Traditionally, HER-2 status has been assessed through immunohistochemical (IHC) staining or fluorescence in situ

Received: 18 July 2025
Accepted: 7 November 2025
Published: 2 December 2025

hybridization (FISH), the gold standard methods for diagnosis.[5–7] However, these techniques are invasive and may not be suitable in cases of multifocal tumors, inaccessible lesions, or patients who cannot undergo biopsy. Furthermore, tumor heterogeneity can pose challenges for accurate assessment using biopsy alone, necessitating alternative, non-invasive approaches for HER-2 evaluation.

In this context, radiomics has emerged as a promising tool. By extracting high-dimensional features from imaging modalities such as magnetic resonance imaging (MRI), radiomics can provide a comprehensive understanding of tumor heterogeneity and its molecular characteristics, including HER-2 expression.[8–11] Several studies have explored the potential of radiomics in predicting HER-2 status using MRI, though many have been limited by small sample sizes and single-center designs.[12,13] These studies often focus on anatomical imaging, while multimodal MRI approaches—combining dynamic contrast-enhanced imaging (DCE-MRI), diffusion-weighted imaging (DWI), and T2-weighted imaging—remain underexplored in this context.

This study aims to address these gaps by developing a radiomics-based nomogram that integrates multimodal MRI features with clinical data to predict HER-2 status in breast cancer. Our results demonstrate that the proposed nomogram, which combines both radiomic features and immune profiling data, significantly enhances the accuracy of HER-2 status prediction compared to traditional imaging methods alone. The inclusion of immune profiling was particularly valuable in capturing the tumor microenvironment's influence on HER-2 expression, offering additional insight into tumor biology.

Methods

Patients' Selection

A total of 320 patients with breast cancer from June 2022 to June 2024 were retrospectively selected as the study subjects in our institution. All patients met the diagnostic criteria for breast cancer according to the National Comprehensive Cancer Network (NCCN) Guidelines for Breast Cancer (2023 edition). Among the cohort, 80 patients were in the HER-2 positive group, and 240 patients were in the HER-2 negative group. The selection of patients included in this study is illustrated in Figure 1. All patients were treated with standard chemotherapy and, if indicated, HER-2-targeted therapy. This study was approved by the ethics committee of Longyan First Affiliated Hospital of Fujian Medical University, All the methods were carried out in accordance with the Declaration of Helsinki. Written informed consent for publication was obtained from all participants prior to their enrollment in the study.

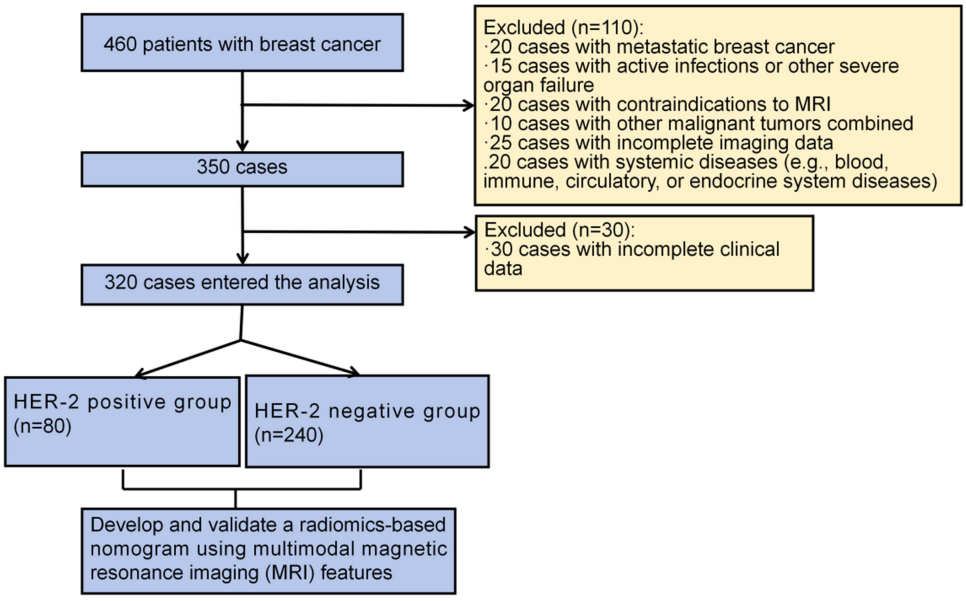

Figure 1 The selection of patients included in this study.

Inclusion Criteria

1) Histologically confirmed invasive breast cancer;[14] 2) Patients with primary tumors (single or multiple) regardless of their size; 3) HER-2 expression status confirmed by immunohistochemical (IHC) staining or fluorescence in situ hybridization (FISH);[15] 4) Availability of pre-treatment multimodal MRI scans, including dynamic contrast-enhanced MRI (DCE-MRI), diffusion-weighted imaging (DWI), and T2-weighted imaging; 5) Patients aged ≥18 years with a Karnofsky performance status score ≥ 70; 6) Patients with complete and standardized medical records, including current and past medical history, laboratory results, and imaging examinations.

Exclusion Criteria

1) Patients with metastatic breast cancer or any history of distant metastasis at the time of diagnosis; 2) Patients with other concurrent malignancies or prior malignancy treated within the past 5 years, except for skin basal cell carcinoma or squamous cell carcinoma; 3) Patients who underwent neoadjuvant therapy prior to enrollment in the study; 4) Patients with contraindications to MRI (eg, pacemakers, metallic implants, or severe claustrophobia); 5) Patients with poor-quality MRI scans or incomplete imaging data; 6) Patients with significant comorbidities such as severe cardiovascular, renal, or hepatic dysfunction that would limit the ability to undergo MRI or other required procedures; 7) Patients with active infections or other severe organ failure; 8) Patients who were unable to cooperate with treatment due to cognitive or psychological impairments.

Definition of Prognosis

In this study, HER-2 positive status was defined as a score of 3+ on IHC or a ratio >2.0 on FISH, in line with established diagnostic criteria.[15] The prognosis was classified based on disease-free survival (DFS) determined from the time of diagnosis to recurrence, metastasis, or the last follow-up. Patients in the HER-2 positive group were compared to those in the HER-2 negative group to assess the predictive accuracy of the radiomics nomogram for HER-2 expression status. Recurrence or metastasis was confirmed through imaging (MRI, CT, or ultrasound) and/or elevated serum biomarkers (eg, CEA, CA 15–3). A good prognosis was defined as patients who remained disease-free during the follow-up period, while a poor prognosis was defined as patients who experienced recurrence or metastasis.

Data Extraction

HER-2 status was primarily determined via histopathological examination using IHC or FISH, the gold standard for assessing HER-2 expression.[15] To address the limitations of repeated biopsies in multifocal tumors or inaccessible lesions, we developed a non-invasive radiomics-based approach using multimodal MRI data.

MRI Acquisition: Pre-treatment MRI scans were acquired using a Philips Ingenia 3.0T scanner with a 16-channel breast-specific coil at Longyan First Affiliated Hospital of Fujian Medical University. Patients were positioned prone with breasts suspended naturally to ensure consistent imaging geometry. Imaging sequences included axial T1-weighted imaging (T1WI), T2WI with fat suppression (T2WI-SPAIR), diffusion-weighted imaging (DWI; b-values: 0, 800 s/mm^2), and dynamic contrast-enhanced MRI (DCE-MRI; eTHRIVE technique, 8 dynamic phases, 60s per phase). Scanning parameters were standardized to minimize variability: T1WI (TR/TE: 5.1/2.3 ms, slice thickness: 1.5 mm), T2WI-SPAIR (TR/TE: 4000/70 ms, slice thickness: 3 mm), DWI (TR/TE: 5000/60 ms, FOV: 340 mm), and DCE-MRI (TR/TE: 4.5/2.2 ms, flip angle: 10°, standardized contrast agent dose: 0.1 mmol/kg gadolinium-based contrast). These sequences captured tumor characteristics (shape, texture, heterogeneity, enhancement patterns) for radiomics analysis. To ensure reproducibility, all scans adhered to a strict institutional protocol with consistent acquisition settings and regular scanner calibration. However, we acknowledge that using a single MRI scanner (Philips Ingenia 3.0T) may limit the generalizability of radiomic features due to potential variability across different manufacturers (eg, GE, Siemens) or scan parameters (eg, DCE contrast agent dose, DWI b-values). This limitation is discussed in Section 4.3, and we emphasize the need for future cross-device validation studies to assess feature robustness across diverse MRI platforms, which is critical for clinical translation.

Radiomics Feature Extraction: Tumor regions of interest (ROIs) were manually segmented on DCE-MRI, DWI, and T2WI by two radiologists (with 8 and 12 years of experience) using ITK-SNAP (v3.8.0). Inter-observer agreement was

assessed via intraclass correlation coefficient (ICC > 0.85). A total of 1,218 radiomic features were extracted using Pyradiomics (v3.0.1), including: 1) First-order features (n=18): Intensity statistics (eg, mean, median, skewness).2) Shape features (n=14): Tumor geometry (eg, volume, surface area). 3) Texture features (n=75): Gray-level co-occurrence matrix (GLCM), gray-level run-length matrix (GLRLM), and gray-level size zone matrix (GLSZM). 4) Higher-order features (n=1,111): Wavelet and Laplacian of Gaussian-filtered features. Features were normalized using z-score standardization to account for scale differences. To ensure reproducibility, images were resampled to a uniform voxel size ($1\times1\times1$ mm^3), and gray-level discretization was applied (bin width: 25).

Feature Selection: To reduce dimensionality and overfitting, a three-step feature selection process was employed: 1) Variance threshold: Features with low variance (< 0.1) were excluded. 2) Correlation analysis: Highly correlated features (Pearson correlation coefficient > 0.8) were removed, retaining the feature with the highest correlation to HER-2 status. 3) LASSO regression: Least Absolute Shrinkage and Selection Operator (LASSO) was used to select the most predictive features, with the regularization parameter (λ) optimized via 10-fold cross-validation. This yielded 12 radiomic features (4 first-order, 3 shape, 5 texture) strongly associated with HER-2 status.

Immune Profiling: Immune profiling was performed to assess the tumor microenvironment's influence on HER-2 expression. Tumor tissue samples were obtained via biopsy or surgical resection. Immunohistochemistry (IHC) was used to quantify immune cell populations, including CD8+ T-cells (cytotoxic T-cells), CD4+ T-cells (helper T-cells), M1 macrophages (anti-tumor), and regulatory T-cells (Tregs, immunosuppressive). Tumor-associated macrophages (TAMs) were assessed using CD68 and CD163 markers. Staining was performed on 4-μm paraffin-embedded sections using standardized antibodies (eg, anti-CD8, clone C8/144B; anti-CD4, clone 4B12). Immune cell density was quantified as the percentage of positive cells per high-power field (×400 magnification) across five representative fields. Serum biomarkers (CEA, CA 15–3, CA 27.29, CYFRA 21–1, AFP, S100) were measured via enzyme-linked immunosorbent assay (ELISA) using commercial kits (eg, Roche Diagnostics) to complement immune profiling and assess tumor behavior.

Data Integration and Validation: Radiomic features, immune profiling data, and clinical variables (eg, age, tumor size, lymph node status) were integrated into a nomogram. Follow-up MRI and biomarker assessments (every 6 months) validated HER-2 status predictions and monitored disease progression. Stable biomarkers and no new lesions indicated unchanged HER-2 status, while progression (new lesions or biomarker elevation) suggested potential recurrence. Only high-quality imaging and complete clinical records were included to ensure data reliability.

Outcome Measures

The primary outcome was HER-2 expression status, determined via IHC (score of 3+ or 2+ with FISH confirmation) or FISH (ratio > 2.0). The secondary outcome was the predictive performance of the radiomics nomogram, integrating multimodal MRI features, immune profiling, and clinical data to estimate HER-2 positivity or negativity. Follow-up imaging (MRI, ultrasound) and serum biomarkers (CEA, CA 15–3) were used to monitor recurrence or progression, defined as new lesions or biomarker elevation. The nomogram's performance was evaluated using predictive accuracy, sensitivity, specificity, and area under the receiver operating characteristic curve (AUC). A good prognosis was defined as disease-free status, while a poor prognosis indicated recurrence or metastasis. Validation compared nomogram predictions with histopathological HER-2 status at baseline.

Immune Profiling Metrics: Immune cell infiltration (CD8+, CD4+, M1 macrophages, Tregs, TAMs) and serum biomarker levels were quantified to assess their correlation with HER-2 status and prognosis. These metrics enhanced the nomogram's ability to capture tumor microenvironment dynamics.

Statistical Analysis

All statistical analyses were performed using R (v4.2.1) and Python (v3.9.5) with the scikit-learn package (v1.0.2). Data normality was assessed using the Shapiro–Wilk test. Continuous variables were compared using the independent *t*-test for normally distributed data or the Mann–Whitney *U*-test for non-normally distributed data. Categorical variables were analyzed using the chi-square test or Fisher's exact test when expected counts were <5. Multivariate logistic regression with Least Absolute Shrinkage and Selection Operator (LASSO) regularization was used to identify independent predictors of HER-2 positivity, incorporating radiomic features, immune profiling metrics (eg, CD8+ T-cell density, TAM percentage), and clinical variables (eg, age, tumor stage). The regularization parameter (λ) was optimized via 10-fold cross-validation. The radiomics

nomogram was constructed using selected predictors, with coefficients derived from the logistic regression model. Model performance was evaluated using the area under the receiver operating characteristic curve (AUC), calibration plots with the Hosmer-Lemeshow test ($p > 0.05$ indicating good fit), and decision curve analysis (DCA) to assess clinical utility across threshold probabilities. Survival analysis was conducted using the Kaplan-Meier method, with differences in disease-free survival (DFS) and overall survival (OS) between HER-2 positive and negative groups compared using the Log rank test. The dataset was divided into training (70%, n=224) and validation (30%, n=96) sets via stratified random sampling to ensure balanced HER-2 status distribution. Internal validation was performed using 10-fold cross-validation, and external validation was conducted on the validation set. Model robustness was assessed via bootstrap resampling (1,000 iterations). Statistical significance was set at $p < 0.05$ (two-tailed).

Results

Comparison of Clinical Characteristics Between Two Groups

No significant differences were observed between the HER-2 positive and negative groups with respect to age, menstrual status, pathological grade, Ki-67 expression, tumor size, or follow-up duration (all $P > 0.05$). However, HER-2 positivity was strongly associated with hormone receptor status: ER negativity was significantly more prevalent in the HER-2 positive group ($P < 0.001$), and PR negativity was also more common ($P = 0.001$) (Table 1).

Comparison of MRI Parameters Between the Two Groups

Compared with HER-2 negative tumors, HER-2 positive lesions more frequently presented as masses (67.5% vs 39.6%) with blurred or ill-defined margins (41.3% vs 15.0%), and were significantly associated with local skin thickening or depression (63.8% vs 48.3%) as well as axillary lymph node abnormalities without overt enlargement (58.8% vs 39.6%) (all $P<0.01$). By contrast, HER-2 negative cancers were more often characterized by non-mass enhancement and smooth margins. No significant intergroup differences were observed in nipple–areola complex involvement, TIC type, or background parenchymal enhancement (Table 2). These findings indicate that HER-2 positive breast cancers exhibit a more aggressive MRI phenotype, with features suggestive of invasive behavior and subclinical nodal involvement.

Table 1 Comparison of Clinical Characteristics Between Two Groups

Clinical Features	HER-2 Positive Group (n=80)	HER-2 Negative Group (n=240)	P
Age	50.56±9.12	49.80±8.83	0.508
Menstrual state			0.078
Menopause	41(51.25%)	96(40.00%)	
Premenopause	39(48.75%)	144(60.00%)	
Pathological grade			0.960
I	6(7.50%)	20(8.33%)	
II	47(58.75%)	142(59.17%)	
III	27(33.75%)	78(32.50%)	
ER			<0.001
Positive	55(68.75%)	80(33.33%)	
Negative	25(31.25%)	160(66.67%)	
PR			0.001
Positive	51(63.75%)	101(42.08%)	
Negative	29(36.25%)	139(57.92%)	
Ki67			0.741
Positive	14(17.50%)	46(19.17%)	
Negative	66(82.50%)	194(80.83%)	
Tumor volume (cm)	6.71±2.30	7.07±1.98	0.174
Follow-up duration (months)	24.81±5.98	24.33±6.96	0.578

Abbreviations ER, Estrogen Receptor; PR, Progesterone Receptor; Ki67, Ki-67 Antigen.

Table 2 Comparison of MRI Parameters Between the Two Groups

MRI Features	HER-2 Positive Group (n=80)	HER-2 Negative Group (n=240)	χ^2	P
Type			18.793	<0.001
Lump	54(67.50%)	95(39.58%)		
Nonmass	26(32.50%)	145(60.42%)		
Edge			24.449	<0.001
Smooth	23(28.75%)	101(42.08%)		
Blur	24(30.00%)	103(42.92%)		
Burr	33(41.25%)	36(15.00%)		
There is no involvement of the nipple areola			3.535	0.060
Yes	29(36.25%)	116(48.33%)		
No	51(63.75%)	124(51.67%)		
Local skin thickening or depression			8.148	0.004
Yes	47(58.75%)	97(40.42%)		
No	33(41.25%)	143(59.58%)		
Axillary lymph nodes without enlargement			18.793	<0.001
Yes	54(67.50%)	95(39.58%)		
No	26(32.50%)	145(60.42%)		
TIC type			0.610	0.737
I	10(12.50%)	36(15.00%)		
II	38(47.50%)	103(42.92%)		
III	32(40.00%)	101(42.08%)		
BPE type			1.811	0.612
Minimum	9(11.25%)	29(12.08%)		
Mild	38(47.50%)	129(53.75%)		
Moderate	25(31.25%)	57(23.75%)		
Remarkable	8(10.00%)	25(10.42%)		

Abbreviations: HER-2, Human epidermal growth factor receptor 2; TIC, Time-signal strength curve; BPE, background enhancement degree.

Prognostic Analysis of HER-2 Expression Level in Breast Cancer Patients

The HER-2 negative group shows a significantly higher PFS compared to the HER-2 positive group (p<0.001). Similarly, the HER-2 negative group exhibits a superior overall survival rate (p<0.001) (Figure 2). These findings suggest that patients in the HER-2 negative group have better survival outcomes in both progression-free survival and overall survival compared to those in the HER-2 positive group.

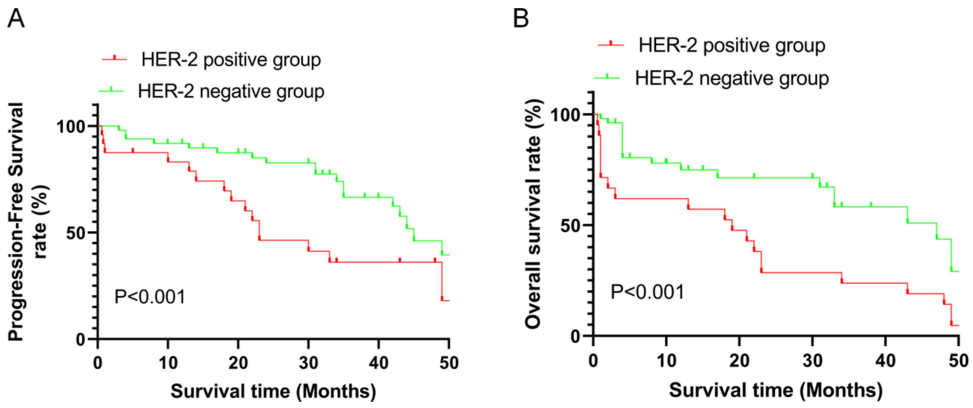

Figure 2 Kaplan-Meier survival curves. (**A**) The progression-free survival rate of different HER-2 status; (**B**) The overall survival rate of different HER-2 status.

The Clinical Baseline Characteristics of the Training Set and the Validation Set

In our study, the patients were divided into a training set (n =280) and a test cohort (n = 40) in a ratio of 7:3, with no statistically significant differences observed across demographic, pathological, or molecular features (all $P > 0.05$). The mean age and menopausal status distribution were comparable between groups, and the pathological grade composition showed a predominance of grade II tumors in both sets. Similarly, the expression profiles of ER, PR, and HER2, as well as Ki-67 status, demonstrated no significant imbalance. Tumor-related parameters, including size, morphology, margin, enhancement pattern, and surface characteristics such as evenness, unevenness, and toroidal configuration, were consistent between the two cohorts, as were peritumoral edema and TIC type (Table 3). Collectively, these results indicate that the training and validation sets were matched in baseline clinicopathological and imaging characteristics, thereby reducing the likelihood of selection bias and supporting the robustness of subsequent model development and validation.

Table 3 The Clinical Baseline Characteristics of the Training Set and the Validation Set

Clinical Features	Training Set (n=280)	Validation Set (n=40)	P
Age	49.82±10.05	48.90±11.32	0.594
Menstrual state			0.866
Menopause	143(51.07%)	21(52.50%)	
Premenopause	137(48.93%)	19(47.50%)	
Pathological grade			0.449
I	23(82.14%)	5(12.50%)	
II	174(62.14%)	21(52.50%)	
III	83(29.64%)	14(35.00%)	
ER			0.786
Positive	90(32.14%)	12(30.00%)	
Negative	190(67.86%)	28(70.00%)	
PR			0.698
Positive	110(39.29%)	17(42.50%)	
Negative	170(60.71%)	23(57.50%)	
HER-2			0.575
Positive	201(71.79%)	27(67.50%)	
Negative	79(28.21%)	13(32.50%)	
Ki67			0.204
Positive	47(16.79%)	10(25.00%)	
Negative	233(83.21%)	30(75.00%)	
Tumor volume (cm)	6.14±2.03	6.27±1.68	0.686
Tumor morphology			0.521
Rule	20(7.14%)	4(10.00%)	
Irregularity	260(92.86%)	36(90.00%)	
Tumor margin			0.211
Smooth	91(32.50%)	17(42.50%)	
Rough	189(67.50%)	23(57.50%)	
Enhance			0.820
Evenness	66(23.57%)	10(25.00%)	
Unevenness	184(65.71%)	27(67.50%)	
Toroidal	30(10.72%)	3(7.50%)	
Peritumoral edema			0.833
Have	142(50.71%)	21(52.50%)	
No	138(49.29%)	19(47.50%)	
TIC type			0.942
I	45(16.07%)	5(12.50%)	
II	80(28.57%)	12(30.00%)	
III	155(55.36%)	23(57.50%)	

Multivariate Analysis

The results of multivariate logistic regression analysis identified Type (OR = 9.660, 95% CI: 3.317–28.139, p < 0.001), Edge (OR = 0.115, 95% CI: 0.043–0.309, p < 0.001), local skin thickening or depression (OR = 0.857, 95% CI: 0.800–0.917, p < 0.001), and axillary lymph nodes with enlargement (OR = 2.905, 95% CI: 2.041–4.135, p < 0.001) as independent risk factors for HER-2 positive breast cancer patients (Table 4). These findings suggest that tumor type confers the greatest risk, followed by axillary lymph node enlargement, whereas irregular edge and local skin thickening or depression act as protective indicators, highlighting the complex interplay of clinicopathological features in predicting HER-2 status.

Development of Nomogram Model

Based on the multivariate logistic regression analysis results, we constructed a nomogram incorporating the independent risk factors (Figure 3). To use this nomogram, the corresponding position on each variable axis was located first according to patient's manifestation. Then, a line was drawn vertically to the points axis above to obtain the respective points. Finally, the points from all four variables were added up, and a line was drawn from the total points axis to the predicted probability axis to estimate the likelihood of HER-2 positive.

Validation of a Nomogram Model

The calibration curves for predicting the risk of HER-2 positive in breast cancer are shown in Figure 4. Figure 4A presents the calibration plot for the training set, while Figure 4B displays the calibration plot for the validation set. The curves illustrate the apparent, bias-corrected, and ideal performance of the nomogram in predicting HER-2 positivity. These results provide a visual comparison of the nomogram's predictive accuracy and the degree of calibration for both datasets. The AUC for the training set was 0.866 (95% CI: 0.760–0.918) (Figure 4C), and the validation set was 0.876 (95% CI: 0.803–0.996) (Figure 4D), it indicated that the nomogram model had a good discrimination and consistency in predicting risk of HER-2 positive in BC.

Decision curve analysis (DCA) demonstrated that if the threshold probability of HER-2 positive in BC was 20 to 75%, the validity of the model was increased (Figure 4E).

Comparison of Tumor Marker Expression Between Two Groups

A comparison of tumor marker expression between the HER-2 positive and HER-2 negative groups revealed significant differences. As depicted in Figure 5, the HER-2 positive group exhibited significantly higher levels of CA15-3, CEA, CA27.29, CYFRA 21–1, AFP, and S100 compared to the HER-2 negative group (p<0.001). These findings highlight that HER-2 positive tumors are characterized by increased expression of markers associated with tumor progression, aggression, and metastatic potential.

Comparative Immune Profiling Between Two Groups

The HER-2 positive group exhibited significantly higher CD8+ T-cell infiltration compared to the HER-2 negative group (p < 0.001), indicating a stronger cytotoxic response. M1 macrophages were also more abundant in HER-2 positive tumors (p < 0.001). Conversely, CD4+ T-cell infiltration showed no significant difference (p>0.05), while Tregs and TAMs were significantly elevated in the HER-2 positive group (p < 0.001 for both) (Figure 6), suggesting a more

Table 4 Multivariate Regression Analysis

Factors	Bate	SE	Wald	OR	95% CI	P
Type	2.268	0.545	17.288	9.660	3.317–28.139	<0.001
Edge	2.165	0.505	18.349	0.115	0.043–0.309	<0.001
Local skin thickening or depression	0.155	0.035	19.863	0.857	0.800–0.917	<0.001
Axillary lymph nodes with enlargement	1.066	0.180	35.059	2.905	2.041–4.135	<0.001

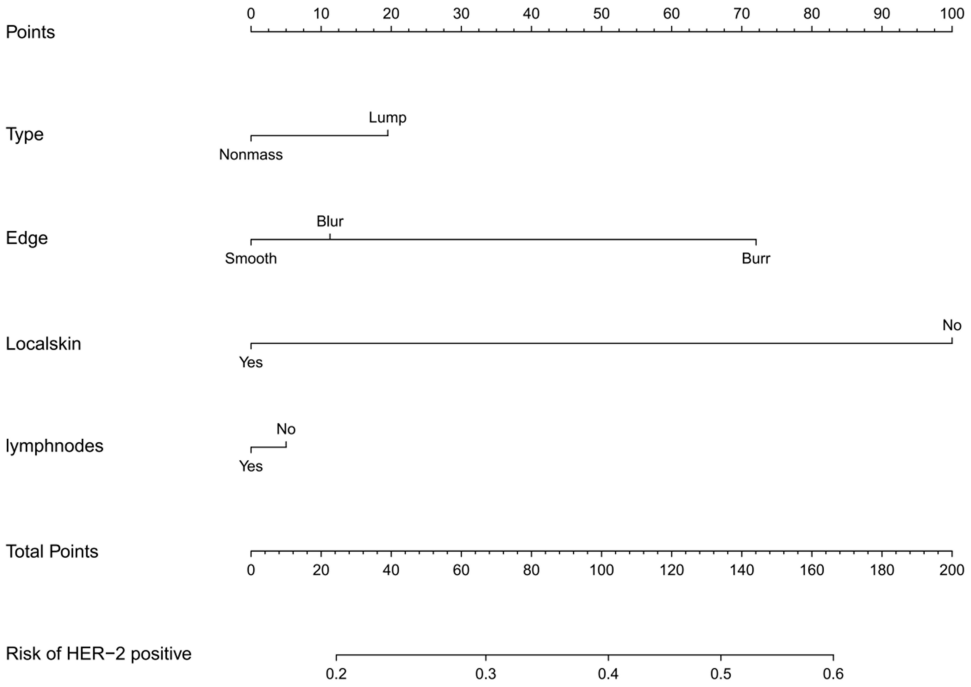

Figure 3 The nomogram for predicting the risk of HER-2 positive in BC.

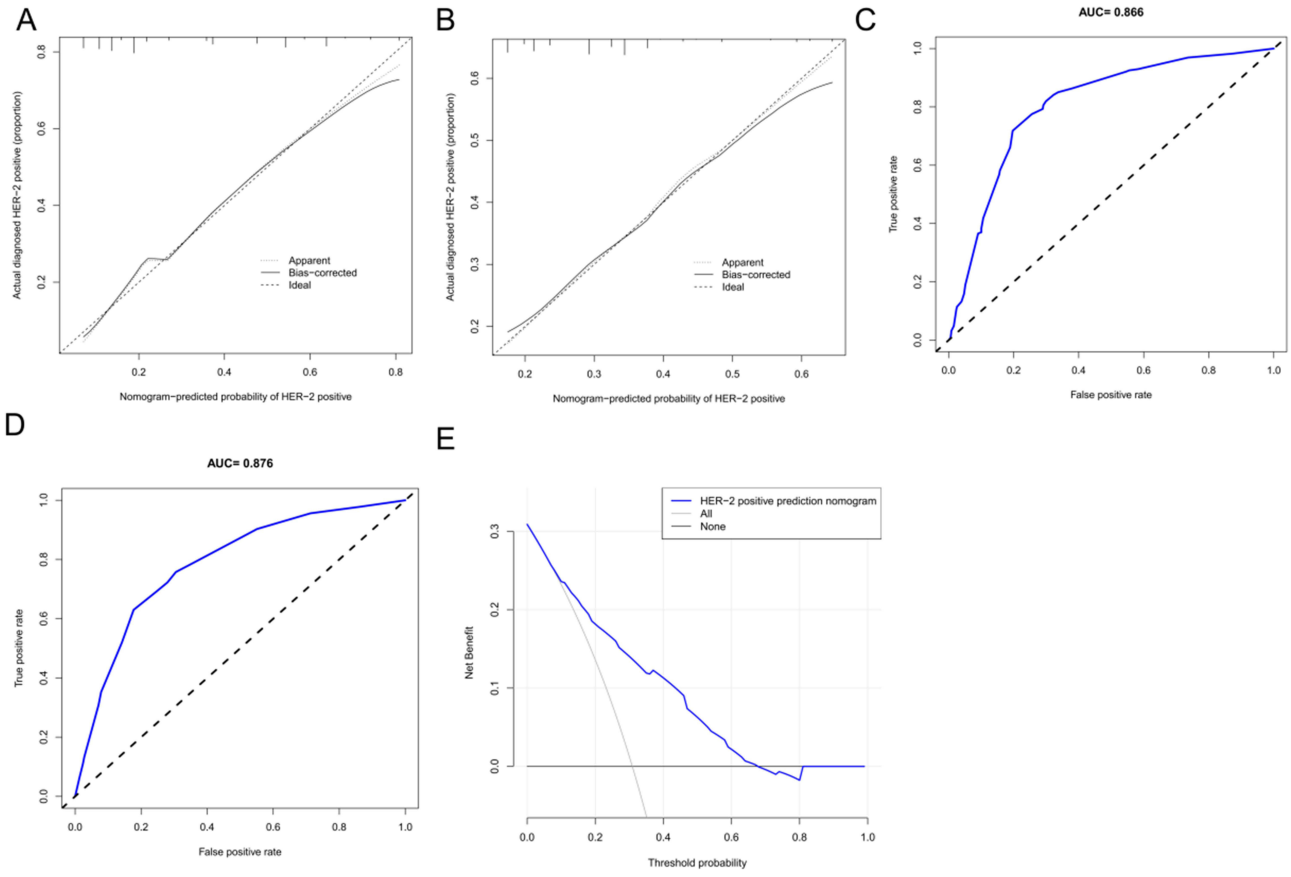

Figure 4 Validation of a nomogram model. (**A**) The calibration curves for the Training set; (**B**) The calibration curves for the Validation set; (**C**) ROC curves for the Training set; (**D**) ROC curves for the Validation set; (**E**) Decision curve analysis for the nomogram.

https://doi.org/10.2147/BCTT.S550088

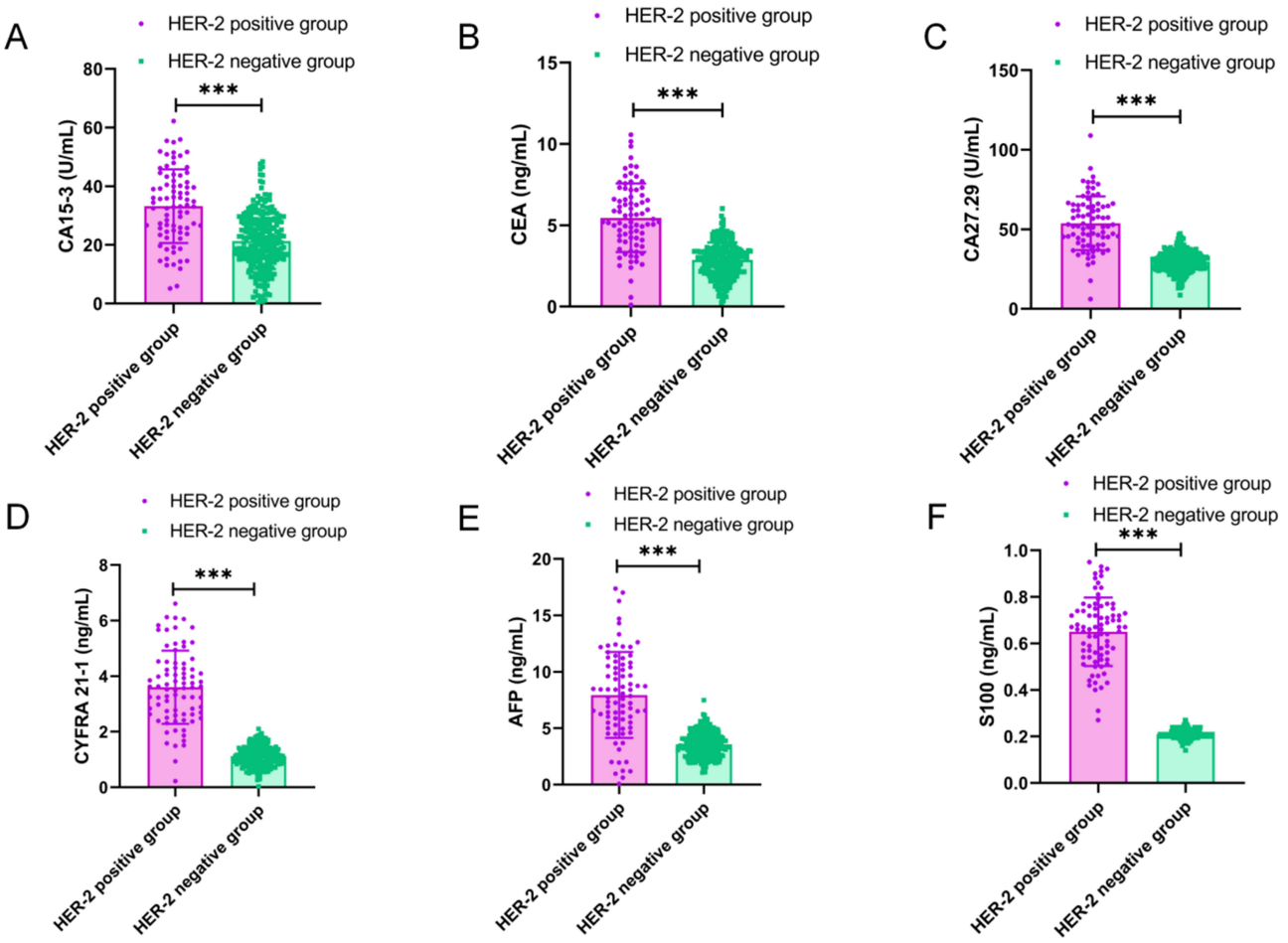

Figure 5 Comparison of Tumor Marker Expression Between Two Groups. (**A**)CA15-3; (**B**) CEA; (**C**) CA27.29; (**D**) CYFRA 21–1; (**E**) AFP; (**F**) S100. Compare to the HER-2 negative group, ***p<0.001.

Abbreviations: CA15-3, Cancer Antigen 15–3; CEA, Carcinoembryonic Antigen; CA27.29, Cancer Antigen 27.29; CYFRA 21–1, Cytokeratin 19 Fragment 21–1; AFP, Alpha-Fetoprotein; S100, S100 Calcium Binding Protein.

immunosuppressive microenvironment. These results highlight distinct immune profiles between the two groups, with HER-2 positive tumors showing an enhanced immune response accompanied by higher levels of immune suppression.

Discussion

Breast cancer, particularly HER-2-positive breast cancer, remains a significant global health concern due to its aggressive nature. HER-2 overexpression is associated with a poor prognosis and increased risk of metastasis, making its accurate prediction vital for guiding personalized treatment strategies, especially with the availability of HER-2-targeted therapies. Traditional methods for determining HER-2 status, such as immunohistochemistry (IHC) and fluorescence in situ hybridization (FISH), are effective but invasive and limited by tumor heterogeneity. Radiomics, using advanced imaging techniques like magnetic resonance imaging (MRI), offers a promising non-invasive alternative for predicting HER-2 expression in breast cancer.

Our findings demonstrate the feasibility of using MRI-based radiomics to predict HER-2 positive. The multivariate logistic regression analysis revealed several clinical and radiomic factors—such as estrogen receptor (ER) positivity, progesterone receptor (PR) positivity, local skin changes, and axillary lymph node enlargement—that are significant independent predictors of HER-2 status. These findings are consistent with previous studies, which suggest that hormonal receptor positivity (ER and PR) is often associated with certain molecular subtypes, including HER-2-positive tumors.[16–19] The correlation between skin changes (such as thickening or depression) and HER-2 positive observed in this study

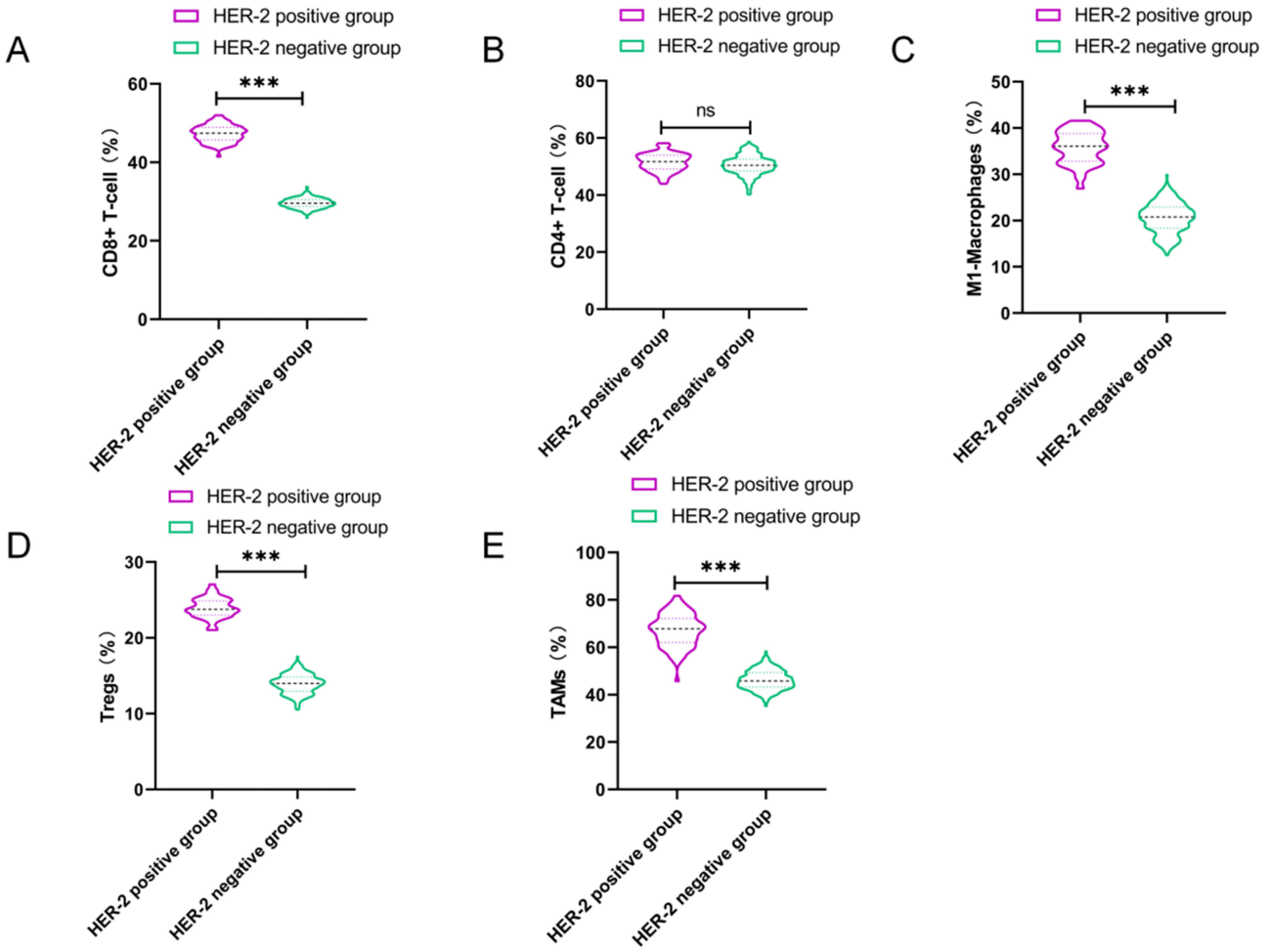

Figure 6 Comparative Immune Profiling Between Two Groups. (**A**) CD8+ T-cell infiltration; (**B**) CD4+ T-cell infiltration; (**C**) M1 Macrophage infiltration; (**D**) Tregs; (**E**) TAMs.Compare to the HER-2 negative group, ***p<0.001, ^{ns}p>0.05.

Abbreviations: CD8+ T-cell, Cytotoxic T Lymphocyte 8+ T-cell; CD4+ T-cell, Helper T-cell 4+ T-cell; M1 Macrophage, M1 Polarized Macrophage; Tregs, Regulatory T-cells; TAMs, Tumor-Associated Macrophages.

aligns with research indicating that HER-2-positive tumors exhibit increased vascularity and aggressive growth.[20,21] These findings underscore the role of MRI in capturing dynamic tumor characteristics non-invasively, which could assist in predicting tumor behavior and aggressiveness.

The detection of local skin thickening or depression via MRI has become a significant feature in assessing tumor aggressiveness. In the context of HER-2 positive breast cancers, these imaging features are indicative of increased tumor vascularity and aggressive growth.[22] The mechanism behind skin changes such as thickening or depression may be attributed to the increased expression of vascular endothelial growth factor (VEGF) and other pro-angiogenic factors typically found in HER-2-positive tumors. HER-2 overexpression is known to upregulate the VEGF pathway, leading to enhanced angiogenesis.[23,24] The associated increase in blood vessel density contributes to the dynamic and sometimes irregular growth patterns of the tumor, which may extend to adjacent tissues, including the skin. These skin changes are also linked to the inflammatory processes often observed in aggressive tumors, further emphasizing the utility of MRI in capturing these dynamic characteristics non-invasively.

Axillary lymph node involvement is a key indicator of breast cancer metastasis and is often associated with poor prognosis.[25] The relationship between axillary lymph node enlargement and HER-2 positive found in our study is supported by the literature, where HER-2 positive tumors tend to be more aggressive and have a higher likelihood of regional and distant metastasis.[26] The mechanistic link between HER-2 expression and lymphatic spread lies in the increased invasiveness of HER-2 positive tumors, which are more likely to penetrate surrounding tissues and invade the

lymphatic system. This enhanced metastatic potential is attributed to the overactivation of signaling pathways such as the phosphoinositide 3-kinase (PI3K)/Akt pathway, which promotes cell migration and invasion.[27] Therefore, the presence of enlarged axillary lymph nodes in HER-2 positive tumors reflects the increased propensity for metastasis, further emphasizing the role of imaging in identifying patients at high risk for aggressive disease.

The integration of multimodal MRI with radiomics analysis offers an innovative and comprehensive approach to predicting HER-2 status without the need for invasive biopsy. Our findings highlight the utility of MRI features—such as texture, shape, and enhancement patterns—as valuable biomarkers for predicting HER-2 positive.[28] These radiomic features capture the tumor's heterogeneity, which is critical for understanding the underlying biology of HER-2 positive tumors. HER-2-positive breast cancers are often more heterogeneous compared to their HER-2-negative counterparts, exhibiting a broader range of histological and molecular features.[29] This heterogeneity can be detected through advanced imaging techniques, where texture and shape features reflect the tumor's microenvironment and structural complexity. Moreover, dynamic contrast-enhanced MRI (DCE-MRI) provides information on tumor vascularity, which is often increased in HER-2 positive cancers due to the upregulation of pro-angiogenic factors like VEGF.[30] This suggests that radiomics, when combined with conventional imaging, can provide a more accurate, non-invasive method of assessing HER-2 expression and guiding therapeutic decisions.

However, it is important to acknowledge certain methodological limitations in our study. First, while we observed a significant association between axillary lymph node enlargement and HER-2 positive, the relationship between lymph node involvement and HER-2 expression is complex and may vary depending on other factors, such as tumor stage and histological subtype. Although previous studies support this correlation, our study cannot definitively establish a causal link between lymph node enlargement and HER-2 expression. Furthermore, while we speculated that immune profiles might play a role in HER-2 prediction, the evidence in our study did not strongly support this hypothesis. The integration of immune profiling into our radiomics model was an exploratory approach, but the relationship between immune responses and HER-2 expression requires further validation and a more robust dataset. Therefore, we recognize the need for additional studies to clarify the potential role of immune profiling in predicting HER-2 status.

The radiomics-based nomogram developed in this study demonstrated excellent predictive performance, with an area under the receiver operating characteristic (ROC) curve (AUC) of 0.866 in the training set and 0.876 in the validation set. This suggests that the nomogram holds promise as a non-invasive tool for predicting HER-2 status, particularly in clinical scenarios where biopsy is not feasible or when dealing with multifocal tumors. By integrating both clinical and MRI-derived radiomic features, the nomogram allows for accurate HER-2 prediction, potentially reducing the need for invasive biopsy procedures, minimizing patient discomfort, and lowering healthcare costs. However, we acknowledge that the relatively small validation cohort limits the generalizability of our findings. Larger, multicenter studies with more diverse patient populations are essential to validate and refine the predictive accuracy of the nomogram. In future work, the integration of molecular biomarkers, such as genetic or proteomic data, could improve the predictive power of the model. Combining radiomics with genomic profiles has the potential to create more personalized and precise predictive models, allowing for more tailored treatment decisions. Additionally, exploring deep learning techniques for radiomic analysis could enhance feature extraction and further improve the precision of HER-2 prediction. The integration of other advanced imaging modalities, such as positron emission tomography (PET), could provide additional insight into tumor metabolism, further complementing the morphological and textural features captured by MRI.

Although the study has shown promising results, we also recognize the limitations of using radiomics alone as a diagnostic tool. While the integration of multimodal MRI offers a non-invasive alternative to biopsy, it is important to emphasize that the model requires further validation in diverse patient populations before widespread clinical adoption. The clinical implementation of this model would benefit from validation in larger and more heterogeneous cohorts, as well as the incorporation of additional factors, such as tumor genomics, to enhance prediction accuracy.

In conclusion, this study demonstrates the potential of using a radiomics-based nomogram, derived from multimodal MRI, for the non-invasive prediction of HER-2 status in breast cancer. The nomogram's ability to integrate clinical and imaging features into a comprehensive predictive model offers a promising tool for personalized treatment planning. Despite its limitations, this approach represents a significant step forward in breast cancer management by reducing the

need for invasive procedures and improving early decision-making. Future studies should focus on validating this model in larger cohorts and exploring the integration of molecular data to further enhance its clinical utility.

Disclosure

The authors report no conflicts of interest in this work.

References

1. Bardia A, Hu X, Dent R. et al. Trastuzumab deruxtecan after endocrine therapy in metastatic breast cancer. *N Engl J Med*. 2024;391 (22):2110–2122. doi:10.1056/NEJMoa2407086
2. Miller KD, Fidler-Benaoudia M, Keegan TH, Hipp HS, Jemal A, Siegel RL. Cancer statistics for adolescents and young adults, 2020. *CA Cancer J Clin*. 2020;70(6):443–459. doi:10.3322/caac.21637
3. Al-Bdour MZ, Al-Shimi R, Al-Rifai MJ, El-Taani H, Nashwan AJ. Navigating human epidermal growth factor receptor 2 (HER2) conversion: insights from recurrent breast cancer. *Cureus*. 2024;16(5):e61305. doi:10.7759/cureus.61305
4. Taori S, Habib A, Adida S, et al. Circulating biomarkers in high-grade gliomas: current insights and future perspectives. *J Neurooncol*. 2025;172 (1):41–49. doi:10.1007/s11060-024-04903-z
5. Kataoka M, Iima M, Miyake KK, Honda M. Multiparametric approach to breast cancer with emphasis on magnetic resonance imaging in the era of personalized breast cancer treatment. *Invest Radiol*. 2024;59(1):26–37. doi:10.1097/RLI.0000000000001044
6. Zhou J, Hou Z, Tian C, et al. Review of tracer kinetic models in evaluation of gliomas using dynamic contrast-enhanced imaging. *Front Oncol*. 2024;14:1380793. doi:10.3389/fonc.2024.1380793
7. Anani T, Rahmati S, Sultana N, David AE. MRI-traceable theranostic nanoparticles for targeted cancer treatment. *Theranostics*. 2021;11 (2):579–601. doi:10.7150/thno.48811
8. Zhou M, Zhou Z, Hu L, et al. Multiplex immunohistochemistry to explore the tumor immune microenvironment in HCC patients with different GPC3 expression. *J Transl Med*. 2025;23(1):88. doi:10.1186/s12967-025-06106-0
9. Choong GM, Cullen GD, O'Sullivan CC. Evolving standards of care and new challenges in the management of HER2-positive breast cancer. *CA Cancer J Clin*. 2020;70(5):355–374. doi:10.3322/caac.21634
10. Ramakrishna N, Anders CK, Lin NU, et al. Management of advanced human epidermal growth factor receptor 2-positive breast cancer and brain metastases: ASCO guideline update. *J Clin Oncol*. 2022;40(23):2636–2655. doi:10.1200/JCO.22.00520
11. Conti A, Duggento A, Indovina I, Guerrisi M, Toschi N. Radiomics in breast cancer classification and prediction. *Semin Cancer Biol*. 2021;72:238–250. doi:10.1016/j.semcancer.2020.04.002
12. Rai R, Barton MB, Chlap P, et al. Repeatability and reproducibility of magnetic resonance imaging-based radiomic features in rectal cancer. *J Med Imaging*. 2022;9(4):044005. doi:10.1117/1.JMI.9.4.044005
13. Bazargani S, Feibus AH, Elshafei A, et al. Magnetic resonance imaging radiomic features for recurrent prostate cancer following proton radiation therapy-A pilot study. *Urol Oncol*. 2023;41(3):145.e1–145.e5. doi:10.1016/j.urolonc.2022.10.007
14. Chen L, Wu Z, Guo C, Wan H, Wu S, Wang G. Triple-negative accessory breast cancer occurring concurrently with primary invasive breast carcinoma: a case report. *Front Surg*. 2024;11:1252131. doi:10.3389/fsurg.2024.1252131
15. Pu X, Li L, Xu F, et al. HER2 amplification subtype intrahepatic cholangiocarcinoma exhibits high mutation burden and T cell exhaustion microenvironment. *J Cancer Res Clin Oncol*. 2024;150(8):403. doi:10.1007/s00432-024-05894-0
16. Mohanty SS, Sahoo CR, Padhy RN. Role of hormone receptors and HER2 as prospective molecular markers for breast cancer: an update. *Genes Dis*. 2022;9(3):648–658. doi:10.1016/j.gendis.2020.12.005
17. Braga FHG, Gómez-Mendoza DP, Lemos RP, et al. Proteomic analysis reveals stage-specific reprogramed metabolism for the primary breast cancer cell lines MGSO-3 and MACL-1. *Proteomics*. 2022;22(17):e2200095. doi:10.1002/pmic.202200095
18. Li JJX, Cheng HY, Lee CHC, Ng JKM, Tsang JY, Tse GM. Single-cell multiplex immunocytochemistry in cell block preparations of metastatic breast cancer confirms sensitivity of GATA-binding protein 3 over gross cystic disease fluid protein 15 and mammaglobin. *Cancer Cytopathol*. 2025;133(1):e22910. doi:10.1002/cncy.22910
19. Van Keymeulen A, Lee MY, Ousset M, et al. Reactivation of multipotency by oncogenic PIK3CA induces breast tumour heterogeneity. *Nature*. 2015;525(7567):119–123. doi:10.1038/nature14665
20. Watson J, Wang T, Ho KL, et al. Human basal-like breast cancer is represented by one of the two mammary tumor subtypes in dogs. *Breast Cancer Res*. 2023;25(1):114. doi:10.1186/s13058-023-01705-5
21. Husni Cangara M, Miskad UA, Masadah R, Nelwan BJ, Wahid S. Gata-3 and KI-67 expression in correlation with molecular subtypes of breast cancer. *Breast Dis*. 2021;40(S1):S27–S31. doi:10.3233/BD-219004
22. Ikejima K, Tokioka S, Yagishita K, et al. Clinicopathological and ultrasound characteristics of breast cancer in BRCA1 and BRCA2 mutation carriers. *J Med Ultrason*. 2023;50(2):213–220. doi:10.1007/s10396-023-01296-w
23. Lee JW, Hur J, Kwon YW, et al. KAI1(CD82) is a key molecule to control angiogenesis and switch angiogenic milieu to quiescent state. *J Hematol Oncol*. 2021;14(1):148. doi:10.1186/s13045-021-01147-6
24. Shen K, Shan Z, Li Y, Ji Z, Zhou L, Lv Z. TFAP2A activates ADAM8 to promote lung adenocarcinoma angiogenesis through the JAK/STAT signaling pathway. *J Biochem Mol Toxicol*. 2025;39(1):e70097. doi:10.1002/jbt.70097
25. Jin R, Luo Z, Jun-Li, et al. USP20 is a predictor of poor prognosis in colorectal cancer and associated with lymph node metastasis, immune infiltration and chemotherapy resistance. *Front Oncol*. 2023;13:1023292. doi:10.3389/fonc.2023.1023292
26. Birkenbeuel JL, Goshtasbi K, Adappa ND, Palmer JN, Tong CCL, Kuan EC. Recurrence rates of de-novo versus inverted papilloma-transformed sinonasal squamous cell carcinoma: a meta-analysis. *Rhinology*. 2022;60(6):402–410. doi:10.4193/Rhin22.187
27. Mansur F, Arshad T, Liska V, Manzoor S. Interleukin-22 promotes the proliferation and migration of hepatocellular carcinoma cells via the phosphoinositide 3-kinase (PI3K/AKT) signaling pathway. *Mol Biol Rep*. 2023;50(7):5957–5967. doi:10.1007/s11033-023-08542-x

28. Fan M, Cheng H, Zhang P, et al. DCE-MRI texture analysis with tumor subregion partitioning for predicting Ki-67 status of estrogen receptor-positive breast cancers. *J Magn Reson Imaging*. 2018;48(1):237–247. doi:10.1002/jmri.25921
29. Li Y, Zhang X, Qiu J, Pang T, Huang L, Zeng Q. Comparisons of p53, KI67 and BRCA1 expressions in patients with different molecular subtypes of breast cancer and their relationships with pathology and prognosis. *J BUON*. 2019;24(6):2361–2368.
30. Yeh JL, Kuo CH, Shih PW, Hsu JH, I-Chen P, Huang YH. Xanthine derivative KMUP-1 ameliorates retinopathy. *Biomed Pharmacother*. 2023;165:115109. doi:10.1016/j.biopha.2023.115109